Corrosion behaviour and surface topography for steel plates used in automotive industry exposed to salty corrosive thermo-accelerated medium

Shaymaa Abbas ABDULSADA ▪ Faculty of Engineering, University of Kufa, Iraq
Ali I. AL-MOSAWI ▪ Institute of Ceramic and Polymer Engineering, University of Miskolc, Hungary
▪ alialmosawi76@gmail.com

Érkezett: 2022. 06. 14. ▪ Received: 14. 06. 2022. ▪ https://doi.org/10.14382/epitoanyag-jsbcm.2022.31

Shaymaa Abbas ABDULSADA
PhD in Metallurgy, Materials Department, Faculty of Engineering, University of Kufa, Iraq. Research Interests: Materials Testing and Processing, Engineering of Metallurgy, Corrosion Engineering, Heat Treatment of Metals, Casting of Metals, Non-Metals Degradation.

Ali I. AL-MOSAWI
PhD in polymers Engineering at Institute of Ceramic and Polymer Engineering, Faculty of Materials Science and Engineering, University of Miskolc, Hungary. Research Interests: Polymers, Composite Materials, Rubber Technology, Flame Retardants, Materials Testing, Materials Processing.

Abstract
Corrosion resistance is one of the essential criteria in the automotive industry, especially in harsh climates, as it causes severe damage to vehicles. Therefore, the anti-corrosion factor should be a complementary and integral part of other safety standards. An experimental investigation for monitoring and evaluating the corrosion behavior of high strength low carbon steel plates with different surface characteristics and treatments conditions used in the automotive industry exposed to a salty, corrosive thermo-accelerated medium has been introduced in this empirical study. The produced samples are divided into four main groups: welded, unwelded, coated, and uncoated. These samples were exposed to an aggressive chemical medium consisting of salty-aqueous spray with a 5% NaCl concentration at 35 °C with speed and pressure. All changes in surface features, including topography, roughness, and corrosion products, were measured and analyzed periodically every 8 hours for 24 hours by scanning electron microscopy, optical microscopy, and CSPM imager surface roughness analysis. The results showed that the coated samples had lower roughness values and lower corrosion products after 24 hours under the salty-aqueous spray test.
Keywords: Automotive corrosion, Salty corrosive medium, Zinc coating, Roughness
Kulcsszavak: Autóipari korrózió, sós korróziós közeg, cinkbevonat, érdesség

1. Introduction

Since the 1930s, rock salt has started to be sprayed on roads in the winter to de-ice and prevention of the formation. Adding salt (or salty solutions) reduces the freezing point of water to below -20°C, where the salt acts as an inhibitor of the ability of water molecules to form solid ice crystals so they remain liquid [1, 2]. Although this method saves thousands of lives and prevents thousands of accidents annually, on the other hand, it has caused pollution and the emergence of many of its adverse effects on plants, insects, aquatic animals, water sources, and wetlands, close to these roads [3-9]. Furthermore, a significant problem has been arisen for cars due to salt spray which is corrosion. Repeated exposure to salt affects the unpainted parts of the car and the painted parts. As the coating layer becomes unstable and micro-holes begin to appear, which allows the penetration of water and its contents of salts, leading to the formation of underneath bubbling up. Eventually, the coating layer begins to flake off. Rusty metal layers appear under it, which will soon flake off and fall, resulting in the holes if not treated [10-14]. Therefore, it is essential to consider the issue of corrosion in vehicles at a level not less than other safety factors such as body stiffness, strength, airbags, crash severity sensing, fuel consumption efficiency, fire resistance, and so on [15-17].

A wide range of metals and alloys are used in the automotive industry, including, steels, aluminium alloys, composite materials, and other lightweight materials, So, according to this diversity, the corrosion behavior varies from one material to another of these materials. Many types of steels are used in the automotive industry, the most common being high-strength steel, with various grades, and mild steel, as shown in the *Fig. 1*, represents the safety cage of Volvo XC60 which indicates the materials used in its manufacture [18-28]. The use of a high-strength steel in the vehicle's body can be increased the capacity for energy absorption and plastic deformation resistance of the component. To maintain weldability and formability of automotive parts, high-strength steel will have a low alloying and carbon content, with several alloying elements such as titanium, copper, vanadium, and niobium, which are added to obtain a strengthened structure [29-33]. Electrochemical reactions mainly cause corrosion in automobiles, in addition to other corrosives such as humidity, temperature, a range of air contaminants like chlorine, sulphur oxides, nitrogen oxides, de-icing salts that are the subject of this study. The steel is immersed in a suitable electrolyte, such as water or road salt, and certain localized anodes and cathodes are created. Electrons move from the anodes to the cathodes during anodic oxidation and cathodic reduction, as seen in *Fig. 2* [34-37]. There are many techniques used for corrosion protection and the most common of which is zinc coating or as it is called galvanization. Coating by Zinc provides good corrosion resistance to steel through cathodic control. The zinc coating layer has an effective adhesion to the steel surface which will improve the corrosion and abrasion resistance due to the characteristics of the galvanizing process. Besides the effectiveness of this technology, it is also considered as low cost and easier to implement compared to other technologies [36, 38-41].

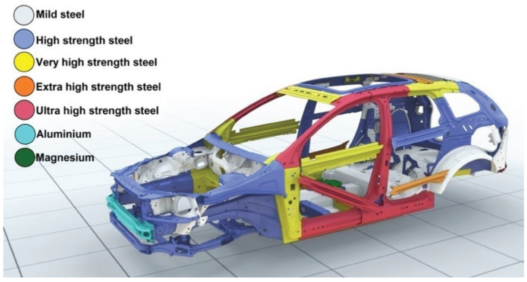

Fig. 1 Materials of Volvo XC60 safety cage [18]
1. ábra A Volvo XC60 biztonságiváz anyagai [18]

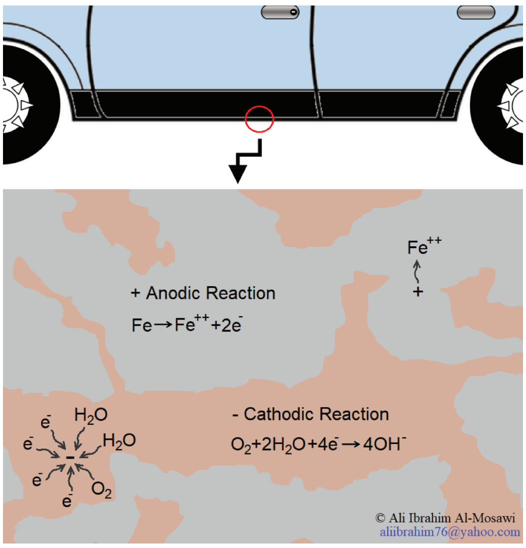

Fig. 2 Corrosion of an automotive body structure
2. ábra Az autóipari karosszéria szerkezetének korróziója

2. Materials and methods

2.1 Materials used

High strength low alloy steel was used in this study. The chemical composition analysis of high-strength low carbon steel shown in *Table 1* was carried out by the ICP-OES method using spectrometer 720 ES.

Chemical composition, %									
C	S	Mn	Si	P	Cr	Ni	Cu	Mo	V
0.07	0.012	0.230	0.140	0.010	0.022	0.036	0.050	0.002	0.003

Table 1 Chemical composition of high strength low alloy steel
1. táblázat Nagy szilárdságú, alacsony ötvözetű acél kémiai összetétele

2.2. Samples preparation

Four samples of high strength low alloy steel (HSLA) plates with dimensions of 5 cm width, 5 cm length, and 1 mm thickness, whose details are illustrated in *Table 2*, were used in this study. The welding process is done using tungsten inert gas arc welding (TIG welding) by Elektra Beckum Industrie WIG 160 DCI. Stress relieving heat treatment was performed at 120 °C for 1 hour, after the cutting and welding process. To provide the optimum surface adhesion, the samples have been cleaned by immersion for 1 min in a dilute HCl mixed with 2 ml of hexamethylenediamine (HMD) corrosion inhibitor to mitigate the effect of HCl on the sample surface upon immersion. After removing the samples from the cleaning solution, they are washed with distilled water, then dried with cotton and placed in a closed container containing a moisture barrier to prevent their oxidation. All sides of the samples are completely coated with a layer of a 200 µm thickness of liquid zinc spray type MAESTRO. The thickness of the coating layer was measured by paint thickness tester PCE-CT 25FN. A summary of the processing steps shown in *Fig. 3*.

Sample	Treatment condition
1	Unwelded and uncoated
2	Unwelded and coated
3	Welded and uncoated
4	Welded and coated

Table 2 Details of test samples
2. táblázat Vizsgálati minták részletezése

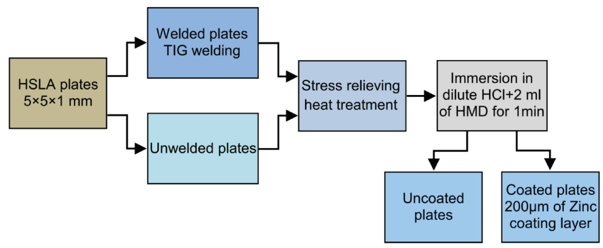

Fig. 3 Processing steps of HSLA plates
3. ábra A HSLA lemezek feldolgozási lépései

2.3 Tests

2.3.1 Salt spray

Thermo-accelerated salt spray test under 5% NaCl salt spray was used to simulate corrosion conditions in natural atmospheres was done according to ISO 9227 [42]. Salt spray cabinet model SF/450 found at University of Miskolc, Hungary was used to complete this test. All surface characteristics of the samples have been recorded before the test started. All surface changes were measured and analyzed during three specific periods, 8, 16, and 24 hours, respectively at 35°C.

2.3.2 Scanning Electron Microscopy (SEM)

This analysis used to determine the spatial distribution of corrosion products on the surface of samples by Carl Zeiss EVO MA10 SEM found at the University of Miskolc in Hungary.

2.3.3 Optical Microscopy

In this surface inspection, Carl Zeiss light optical microscopy with a magnification of 50x was used to detect the extent and spatial distribution of rust, and secondary precipitated phases at the surface of the samples.

2.3.4 Surface roughness

The CSPM imager program shown in *Fig. 4* has been used to surface roughness mapping and evaluation parameters. The investigated surface roughness parameters were mainly the average of the roughness profile (Sa) and core roughness depth (Sk). This superficial evaluation was done according to ISO 21920 for profiles [43, 44] and ISO 25178 for 3D measurements [45].

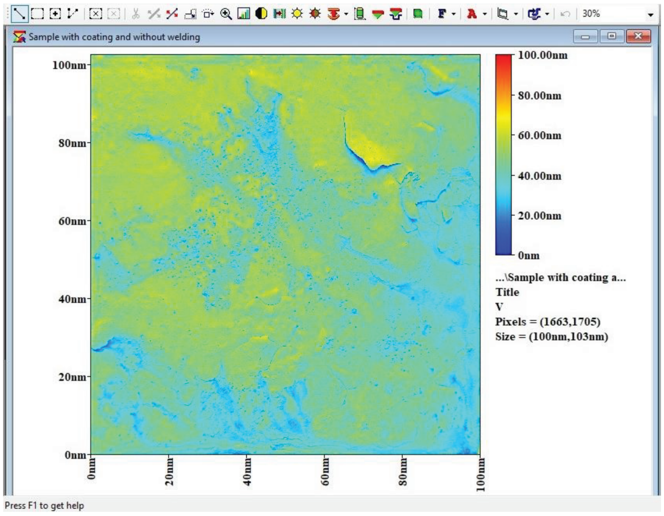

Fig. 4 The CSPM imager program
4. ábra A CSPM imager program

3.Results and Disscusion

3.1 SEM analyses for Surface corrosion products

In such an artificial environment with precipitating salty water with 5% NaCl that mimic the natural conditions of corrosion, HSLA steel plates start corroding in the aqueous salt solution containing dissolved oxygen according to electrochemical reaction mechanism, therefore, there will be migrating tiny local anode and cathode sites with iron dissolution (which will oxidized to ions) and oxygen reduction, respectively. Then the iron(II) and iron(III) cations can react with the anions (first of all OH- anions) present nearby with the formation of soluble and non-soluble oxide-hydroxides and other corrosion products depending on the actual local electrochemical reactions and physical transport circum- stances (diffusion, the solution flows, etc.) [46]. Surface inspection of the samples after exposure to 5% NaCl salt spray for 24 hours has been accomplished by SEM-EDX analysis, and the details are shown in *Fig. 5* and *Fig. 6*, respectively. The corrosion products of this process are listed as oxides in *Table 3*. In *Fig. 5*, the unwelded and uncoated sample showed a severe oxidized surface state that extended over most of the surface, and this state is very clear in *Fig. 6* as well. The chemical composition of this oxidized surface contained about 86.53 wt.% FeO. The analysis also showed that the surface of the unwelded and uncoated sample contained some compound-bound chlorine (Cl_2O) with a quantity of 10.55 wt.%. This indicates that the chloride ions migrated or penetrated the steel surface. Since the chloride ions can quickly and easily dissipates because this sample does not have any protective layer. These ions will initiate and/or develop their corrosion layer through the possible subsequent formation of various iron-oxide-hydroxide (rust) compounds.

In the unwelded and coated sample, the oxidized surface state was reduced by 94.5%, where the FeO content has been decreased from 86.53 wt.% to only 4.75 wt.%. The FeO formation on the coated sample surface is because of the possibility of creating microcracks in the areas of invisible defects of the zinc coating layer resulting from the attack of chloride ions. Thus, the speed of the salt spray helped in the penetration of the saline solution inside the zinc coating layer and thus led to the destroyed (i.e., chemically modified and dissolved away) and peeling of parts of this protective layer. Because of this, the chloride ions content in the oxidized surface was 1.86 wt.%, which is also reduced by 82.4% of what it was in the uncoated sample. As for the welded-uncoated sample, we can notice an increase in the FeO value to 87.95wt.%, which is higher than the unwelded-uncoated sample value, as this sample did not withstand the attack of chloride ions, where the Cl_2O was high (9.96 wt.%) as well as the extension of the oxidized surface to include the welding area as well as shown also in *Fig. 6*, although carry out a stress removal treatment to get rid of the heat-affected zone (HAZ). It is possible that this is related to the presence of some micro-defects in the welding area results from the inefficiency of the welding process entirely along with the sample, which caused the appearance of rust in the welding surface.

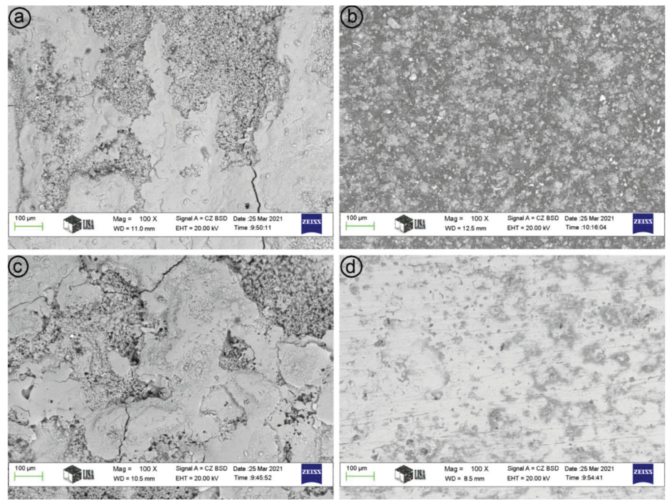

Fig. 5 SEM analysis for HSLA steel plates after exposure to 5% NaCl salt spray for 24 hours, (a) unwelded and uncoated sample, (b) unwelded and coated sample, (c) welded and uncoated sample, and (d) welded and coated sample
5. ábra A korroziós teszt után (24 óra, 5%-os NaCl sópermet) a HSLA acéllemezek SEM-elemzése: (a) hegesztés és bevonat nélküli minta, (b) hegesztés nélküli bevonatos minta, (c) hegesztett bevonat nélküli minta, (d) hegesztett és bevonatos minta

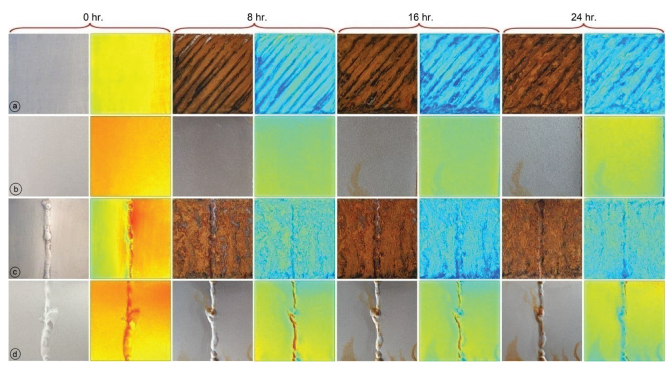

Fig 6. Surface topography and roughness measurements of high strength low alloy steel after 24 hours of exposure to 5% NaCl salt spray, (a) unwelded and uncoated sample, (b) unwelded and coated sample, (c) welded and uncoated sample, and (d) welded and coated sample
6. ábra HSLA acéllemezek felületi topográfiájának és érdességének mérési eredményei a korroziós teszt után (24 óra, 5%-os NaCl sópermet): (a) hegesztés és bevonat nélküli minta, (b) hegesztés nélküli bevonatos minta, (c) hegesztett bevonat nélküli minta,(d) hegesztett és bevonatos minta.

Components	EDX composition analysis, wt%			
	a	b	c	d
Cl_2O	10.55	1.86	9.96	2.99
SiO_2	2.25	1.75	1.54	1.5
MnO	0.67	0.76	0.55	0.94
FeO	86.53	4.75	87.95	6.98
ZnO	-	74.65	-	72.36

Table 3. The chemical composition of HSLA steel samples at different test durations under 5% NaCl salt spray analyzed by SEM-EDS, (a) unwelded-uncoated sample, (b) unwelded-coated sample, (c) welded-uncoated sample, and (d) welded-coated sample

3. táblázat HSLA acélminták kémiai összetétele SEM-EDS elemzéssel 5%-os NaCl sópermet után: (a) hegesztés és bevonat nélküli minta, (b) hegesztés nélküli bevonatos minta, (c) hegesztett bevonat nélküli minta, (d) hegesztett és bevonatos minta.

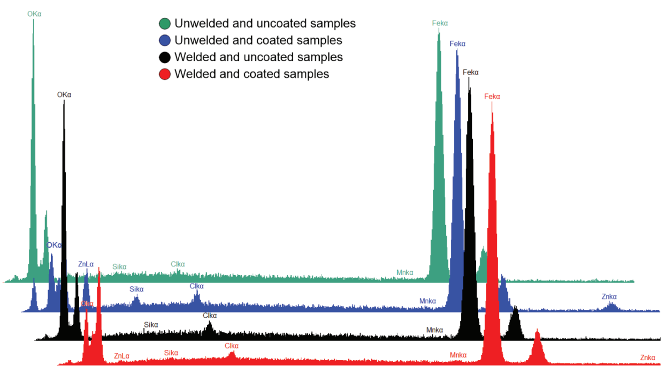

Fig. 7 EDX mapping analysis for HSLA steel plates
7. ábra HSLA acéllemezek EDX elemzése

As for the welded-coated sample, the oxidized surface was higher than in the unwelded-coated sample, where the FeO content was (6.98 wt.%) as we note from *Fig. 7* that despite the coating, the welding area has also oxidized. The reason for this is the rapid appearance of microcracks in the coating layer that covers the welding area, because it is uneven, so the superficial protuberances, no matter how small, will be prone to peeling the paint layer off it and being attacked by chloride ions. Therefore, we see that the proportion of Cl_2O is also high (2.99 wt.%) when compared with the Cl_2O proportion of the unwelded-coated sample. The EDS analysis of HSLA steel plates is shown in *Fig. 7*. Rust is made up of a variety of oxides, including hydrated oxides, oxyhydroxides, and other crystalline and amorphous compounds, although the major components are iron and oxide. As a result, determining the oxygen ratio in the rust layer can provide insight on corrosion process under similar exposure conditions. To further understand the initial corrosion, the chemical composition of the rust layer was examined after 24 hours period of salt spray exposure at typical locations and showed several corroded regions. General corrosion developed throughout the area, as seen in *Fig. 5*, and *Fig. 6*. Corrosion progressed in the sample un welded- uncoated and in the welded and uncoated sample, that was conformed also by peaks of oxygen in EDS analysis. The overall decrease in the corrosion rate in the samples with coating suggests that the corrosion delay was due to the Zinc coating layer because it decrease the harmful attack of chlorides. Corrosion in welded-uncoated sample in reality, when comparing the corrosion in the weld and HAZ zones, these zones is more severe due to the thermal effect because the welding temperature and these with effect of chlorides it will be weak to resist the corrosion [47].

3.2. Monitoring and evaluation of optical micrographs for the surface

Light optical micrographs for the surface of samples are presented in *Fig. 8*. The visual examination revealed that the corrosion initiated and started on the whole surface area of unwelded-uncoated and welded-uncoated samples. Inspection of the unwelded-coated and welded-coated samples upon corrosion initiation typically revealed one distinct corroding spot, which in some cases was surrounded by significantly smaller corrosion pits on the coating layer. The small corrosion pits were interpreted as micro defects where corrosion had initiated but could not reach stable pit growth (in contrast to the dominating corrosion state).

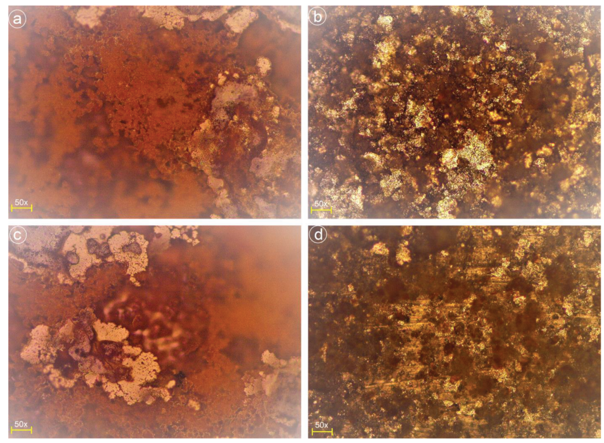

Fig. 8 Light optical micrographs of HSLA steel plates after 24 hours of exposure to 5% NaCl salt spray, (a) unwelded and uncoated sample, (b) unwelded and coated sample, (c) welded and uncoated sample, and (d) welded and coated sample

8. ábra A korróziós teszt után (24 óra, 5%-os NaCl sópermet) a HSLA acéllemezek fénymikroszkópos felvételei: (a) hegesztés és bevonat nélküli minta, (b) hegesztés nélküli bevonatos minta, (c) hegesztett bevonat nélküli minta, (d) hegesztett és bevonatos minta

3.3 Surface topography changes in roughness

The change in surface roughness on the HSLA steel plates surface was mentioned in *Fig. 6*. Before the salt spray test, the surface of the samples has a typical ground topography. However, this simple regular surface pattern soon changes, where more irregular surface and complex topography appear, depending on the type of sample and the duration of exposure to the saline solution. This new topography represents rust, as well as changes to the coating layer. In the stage of the appearance of rust and the effect of the coating layer due to saline solution, the surface roughness will change drastically, as its values will rise, as expected, as shown in the *Fig. 9* and *10*, which represent roughness average and core roughness depth respectively. Uncoated samples generally have the highest roughness rates, and welded samples are the highest despite being coated. Unwelded and coated sample showed the lower roughness values during the different test durations under 5% NaCl salt spray; also welded and coated sample showed slightly higher roughness values comparing with sample unwelded one. These samples (coated) appeared good resistance for corrosion after 24 hours under 5% NaCl salt spray because the zinc coating layer improved the ability to resist the attack of chloride ions and that will lead to progress in the corrosion process slowly. In addition, the values of the roughness depth parameters (Sk) are on average more than twice as high as their roughness average equivalent

(Sa) on the corroded surfaces. One possible reason for this can be that the corrosion appears crater-like at certain points on the surface and therefore has a high surface in homogeneity, which is better detected by roughness depth characteristics.

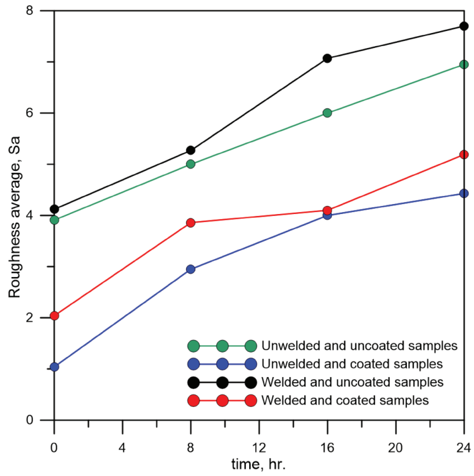

Fig. 9 Roughness average (Sa) values for HSLA steel plates at different test durations under 5% NaCl salt spray
9. ábra Különböző idejű sópermet (5% -os NaCl) teszt után a HSLA acélemezek átlagérdessége (Sa)

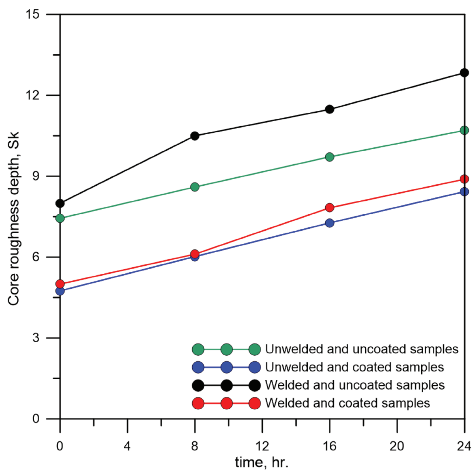

Fig. 10 Core roughness depth (Sk) values for HSLA steel plates at different test durations under 5% NaCl salt spray
10. ábra Különböző idejű sópermet (5% -os NaCl) teszt után a HSLA acélemezek magmagassága (Sk)

4. Conclusions

The oxidized areas spread on the whole surface of the uncoated samples after 8 hours after exposure to the salt spray; this chemical attack also caused significant changes in the surface topography. The percentage of zinc compounds in the case of unwelded-coated samples was higher than that of welded-coated samples by 3.07%, indicating that part of the coating layer has peeled off the welding area, which contributed to its exposure to the attack of chloride ions. Corrosion points appear on the weld area extensively even though they are coated, and stress relieving heat treatment is applied. We believe this behavior may result from the inefficiency of the welding process along the welded surface through the appearance of micro-cracks after welding or the entry of oxygen due to the shallowness of the inert gas which caused poor insulation and full enclosing of the welding area from the outside atmosphere. Therefore, manufacturers must pay attention to these areas and ensure the total efficiency of the welding to provide maximum safety in vehicles. The lowest rates of surface roughness were in the unwelded and coated samples, where the roughness of these samples was less than the welded and coated samples by 17.2% and 5.5% for the roughness average and core roughness depth, respectively. Also, the intensity of the roughness rate after exposure to salt spray varies in the case of the unwelded-uncoated samples and welded-uncoated samples, where the roughness average and core roughness depth were higher in the case of welded-uncoated by 10.8% and 20, respectively than unwelded-uncoated samples, after 24 hours exposure to the saline spray. Concentrations of oxygen and iron oxide (FeO) in welded samples, whether coated or uncoated, are higher than those unwelded ones, which indicates that the salt spray has been penetrated the coating layer earlier than the unwelded ones. The irregular diverse topography of the welding area plays a pivotal role in increasing the coating removal rate from them, making this area susceptible to corrosion, and this is also observed from the low content of ZnO in the welded samples, which is 3.16% less than its unwelded-coated counterparts.

Acknowledgements

We would like to extend our thanks and appreciation to Mr. Lassú Gábor and Mr. Kovács Árpád at the University of Miskolc for their valuable help in salt spray test and SEM measurements.

Reference

[1] Vengosh A., Salinization and saline environments, Chapter 9, In Holland, H.D., Turekian, K.K. (eds.) Treatise on Geochemistry, 2nd edition, Volume 11: Environmental Geochemistry, Elsevier Ltd., pp. 325-378, (2014). https://doi.org/10.1016/B978-0-08-095975-7.00909-8
[2] Kelly V.R., Findlay S.E.G., Schlesinger W.H., Menking K., Morrill A., Road salt moving toward the solution, Special Report, Cary Institute of Ecosystem Studies, USA, (2010). https://www.caryinstitute.org/sites/default/files/public/reprints/report_road_salt_2010.pdf
[3] Evans M., Frick Ch., The effects of road salts on aquatic ecosystems, National Water Research Institute, Series No. 02-308, Canada, (2001). http://scec.ca/pdf/the_effects_road_salts.pdf
[4] Green S.M., Machin R., Cresser M.S., Effect of long-term changes in soil chemistry induced by road salt applications on N-transformations in roadside soils, Environmental Pollution, Vol.152, Issue.1, pp.20-31, (2008). https://doi.org/10.1016/j.envpol.2007.06.005
[5] Novotny E., Murphy D., Stefan H., Road salt effects on the water quality of lakes in the twin cities metropolitan area, St. Anthony Falls Laboratory, Project Report No. 505, Minneapolis, Minnesota, (2007). https://conservancy.umn.edu/bitstream/handle/11299/115334/1/pr505.pdf
[6] Hintz W.D., Fay L., Relyea R.A., Road salts, human safety, and the rising salinity of our fresh waters, Frontiers in Ecology and the Environment,Vol.20, Issue.1, pp.22-30, (2022). https://doi.org/10.1002/fee.2433
[7] Kostka A., Strzebońska M., Sobczyk M., Zakrzewska M., Bochenek A., The effect of de-icing roads with salt on the environment in Krakow (Poland), Geology, Geophysics & Environment, Vol.45, Issue.3, pp.195-205, (2019). https://doi.org/10.7494/geol.2019.45.3.195
[8] Szklarek S., Górecka A., Wojtal-Frankiewicz A., The effects of road salt on freshwater ecosystems and solutions for mitigating chloride pollution - A review, Science of The Total Environment, Vol.805, pp.150289, (2022). https://doi.org/10.1016/j.scitotenv.2021.150289
[9] Wrochna M., Małecka-Przybysz M., Gawrońska H., Effect of road de-icing saltswith anti corrosion agents on selected plant species, Acta Scientiarum Polonorum, Hortorum Cultus, Vol.9, No.4, pp.171-182, (2010). https://czasopisma.up.lublin.pl/index.php/asphc/article/view/3442

[10] Hernandez B., The Effects of road salt on cars & how to protect your vehicle from salt damage, Brian's Auto Detailing, LLC, (2019). https://www.briansautodetailing.com/post/the-effects-of-road-salt-on-cars-how-to-protect-your-vehicle-from-salt-damage

[11] Buchheit R.G., Corrosion resistant coatings and paints, In: Kutz M. (ed.) Handbook of environmental degradation of materials, 2nd edition, William Andrew, USA, pp. 539-568, (2013). https://doi.org/10.1016/B978-1-4377-3455-3.00018-3

[12] Wood F.O., Motor-vehicle corrosion from deicing salt, Transportation Research Record, Vol.762, pp.32-36, (1980). https://onlinepubs.trb.org/Onlinepubs/trr/1980/762/762-007.pdf

[13] Petkuviene J., Paliulis D., Experimental research of road maintenance salts and molasses ("safecote") corrosive impact on metals, Journal of Environmental Engineering and Landscape Management, Vol.17, Issue.4, pp.236-243, (2009). https://doi.org/10.3846/1648-6897.2009.17.236-243

[14] Xi Y., Olsgar P. J., Effects of de-icing agents (magnesium chloride and sodium chloride) on corrosion of truck components, Report No. CDOT-DTD-R-00-10, Colorado Department of Transportatio, USA, (2000). https://www.codot.gov/programs/research/pdfs/2000/truckcomponents.pdf

[15] ISO 26262, Road vehicles-functional safety, International Organization for Standardization-ISO, (2018). https://www.iso.org/obp/ui/#iso:std:iso:26262:-1:ed-2:v1:en

[16] Solonshchikov P., Moshonkin A., Determination of safety parameters for cars and tractors, Transportation Research Procedia, Volume 61, pp.492-498, (2022). https://doi.org/10.1016/j.trpro.2022.01.080

[17] Kitagawa Y., Pal Ch., Evaluation of vehicle body stiffness and strength for car to car compatibility, SAE Technical Paper 2001-01-3098, (2001). https://doi.org/10.4271/2001-01-3098.

[18] Volvo XC60 safety cage, Volvo Car Corporation, (2009). https://www.media.volvocars.com/global/en-gb/media/photos/14629

[19] Vasilash G.S., The Volvo XC60: Stylish, Swedish & Safe, Technical Report, Gardner Business Media, Inc., (2009). https://www.gardnerweb.com/articles/the-volvo-xc60-stylish-swedish-safe

[20] Arno J., Matthias B., New cars-new materials, materials & design, Vol.18, Issues.4-6, pp.203-209, (1997). https://doi.org/10.1016/S0261-3069(97)00049-6

[21] Cheon S. S., Lee D. G., Jeong K. S., Composite side door impact beams for passenger cars, Composite Structures, Vol.38, Issues.1-4, pp.229-239, (1997). https://doi.org/10.1016/S0263-8223(97)00058-5

[22] Sivanura K., Umananda K.V., Pai D., Advanced materials used in automotive industry-a review, AIP Conference Proceedings, Vol.2317, pp.020032, (2021). https://doi.org/10.1063/5.0036149

[23] Abdulsada Sh.A., Corrosion inhibitors :principles and application, 1st Edition, LAP- LAMBERT Academic Publishing, Germany, (2014).

[24] Henriksson F., Introducing new materials in the automotive industry-managing the complexity of introducing new materials in existing production systems, Ph.D. dissertation, Linköping University, Sweden, (2017). https://liu.diva-portal.org/smash/get/diva2:1155571/FULLTEXT02.pdf

[25] Johnson M.C., Sullivan J.L., Lightweight materials for automotive application: an assessment of material production data for magnesium and carbon fiber, Technical Report, Argonne National Laboratory, USA, (2014). https://doi.org/10.2172/1172026

[26] Abdulsada Sh.A., Al-Mosawi A.I., Hadi A.A., studying the effect of eco-addition inhibitors on corrosion resistance of reinforced concrete, Bioprocess Engineering, Vol.1, No.1, pp.81-86, (2017). https://doi.org/10.11648/j.be.20170103.14

[27] Hovorun T. P., Berladir K.V., Pererva V.I., Rudenko S.G., Martynov A. I., Modern materials for automotive industry, Journal of Engineering Sciences, Vol.4, Issue.2, pp. F8-F18, (2017). https://doi.org/10.21272/jes.2017.4(2).f8

[28] Al-Sultani K.F., Abdulsada Sh.A., Improvement corrosion resistance of low carbon steel by using natural corrosion inhibitor, International Journal of Advanced Research, Vol.1, Issue.6, pp. 239-243, (2013). https://www.journalijar.com/uploads/2013-06-26_160757_152.pdf

[29] Hosking N.C., Next generation corrosion protection for the automotive industry, PhD dissertation, University of Nottingham, Uk, (2007). http://eprints.nottingham.ac.uk/14514/1/585527.pdf

[30] Hall J.N., Fekete J.R., Steels for auto bodies: a general overview, In: Rana, R., Singh, S.B. (eds.) Automotive steels: design, metallurgy, processing and applications, Woodhead Publishing, USA, pp. 19-45, (2017). https://doi.org/10.1016/B978-0-08-100638-2.00002-X

[40] Samek L., Krizan D., Steel - material of choice for automotive lightweight applications, 21st International Conference on Metallurgy and Materials, Brno, Czech Republic, , pp.1-6, (2012). http://metal2012.tanger.cz/files/proceedings/02/reports/551.pdf

[41] Li Y., Lin Z., Jiang A., Chen G., Use of high strength steel sheet for lightweight and crashworthy car body, Materials and Design Vol.24, Issue.3, pp.177-182, (2003). https://doi.org/10.1016/S0261-3069(03)00021-9

[42] Cornette D., Hourman T., Hudin O., Laurent J., Reynaert A., High strength steels for automotive safety parts, SAE 2001World Congerss, Detroit, Michigan, USA, pp.0078, (2001). https://doi.org/10.4271/2001-01-0078.

[43] Abdulsada Sh.A., Al-Mosawi A.I., Török T.I., Testing the inhibition potential of fenugreek seed powders on steel rebar samples immersed in aqueous NaCl solution, Proceedings of MultiScience - XXXI. MicroCAD International Multidisciplinary Scientific Conference, University of Miskolc, Hungary, 2017, pp.1-6, (2017). https://doi.org/10.26649/musci.2017.026

[44] Schulz U., Trubiroha P., Schernau U., Baumgart H., The effects of acid rain on the appearance of automotive paint systems studied outdoors and in a new artificial weathering test, Progress in Organic Coatings, Vol.40, Issue.1-4, pp.151-165, (2000). https://doi.org/10.1016/S0300-9440(00)00138-7

[45] Akafuah N.K., Poozesh S., Salaimeh A., Patrick G., Lawler K., Saito K., Evolution of the automotive body coating process-a review, Coatings, Vol.6, Issue.2, 2016, pp.24, (2016). https://doi.org/10.3390/coatings6020024

[46] Abdulsada Sh.A., Török T.I., Fazakas É., Preliminary corrosion testing of steel rebar samples in 3.5% NaCl solution with and without a green inhibitor, Építőanyag-Journal of Silicate Based and Composite Materials, Vol.70, No.2, pp. 48-53, (2018). https://doi.org/10.14382/epitoanyag-jsbcm.2018.10

[47] Zinc coatings: a comparative analysis of process and performance characteristics, Technical Report, American Galvanizers Association, (2011). https://galvanizeit.org/uploads/publications/Zinc_Coatings.pdf

[48] Rocca E., Jacques S., Electrochemical coating of zinc carboxylate: a new protection for Zinc in atmospheric conditions, Surface and Coatings Technology, Vol.429, pp.127940, (2022). https://doi.org/10.1016/j.surfcoat.2021.127940

[49] Amirudin A., Thierry D., Corrosion mechanisms of phosphated zinc layers on steel as substrates for automotive coatings, Progress in Organic Coatings, Vol.28, Issue.1, pp.59-75, (1996). https://doi.org/10.1016/0300-9440(95)00554-4

[50] Petrova L., Demin P., Kolenko N., Luzhnov Y., Increasing the reliability of low-carbon cold-resistant steel elements by diffusion zinc coating methods, Transportation Research Procedia, Vol.57, pp.421-429, (2021). https://doi.org/10.1016/j.trpro.2021.09.069

[51] ISO 9227-3, Corrosion tests in artificial atmospheres- salt spray tests, Switzerland, International Organization for Standardization-ISO, (2017).

[52] ISO 21920-2, Geometrical product specifications (GPS) -Surface texture: Profile -Part 2: Terms, definitions and surface texture parameters, Switzerland, International Organization for Standardization-ISO, (2021). https://www.iso.org/obp/ui/#iso:std:iso:21920:-2:ed-1:v2:en

[53] ISO 21920-3, Geometrical product specifications (GPS)-Surface texture: Profile- Part 3: Specification operators, Switzerland, International Organization for Standardization-ISO, (2021). https://www.iso.org/obp/ui/#iso:std:iso:21920:-3:ed-1:v1:en

[54] ISO 25178-2, Geometrical product specifications (GPS)- Surface texture: Areal- Part 2: Terms, definitions and surface texture parameters, Switzerland, International Organization for Standardization-ISO, (2021). https://www.iso.org/obp/ui/#iso:std:iso:25178:-2:ed-1:v1:en

[55] Alcántara J., Fuente D., Chico B., Simancas J., Díaz I., Morcillo M., Marine atmospheric corrosion of carbon steel: a review, Materials, Vol. 10, Issue. 4, 2017, pp.406, (2017). https://doi.org/10.3390/ma10040406

[56] Choi Y.Y., Kim M.H., Corrosion behaviour of welded low-carbon steel in the arctic marine environment, RSC Advances, Vol.8, Issue.53, pp. 30155-30162, (2018). https://doi.org/10.1039/C8RA05371E

Ref.:
Abdulsada, Shaymaa Abbas– **Al-Mosawi**, Ali I.: *Corrosion behaviour and surface topography for steel plates used in automotive industry exposed to salty corrosive thermo-accelerated medium*
Építőanyag – Journal of Silicate Based and Composite Materials, Vol. 74, No. 6 (2022), 218–223. p.
https://doi.org/10.14382/epitoanyag-jsbcm.2022.31